

Incompressible Lifting-Surface Aerodynamics for a Rotor- Stator Combination

Sridhar M. Ramachandra
*Lewis Research Center
Cleveland, Ohio*

LIBRARY COPY

JAN 2 1985

LANGLEY RESEARCH CENTER
LIBRARY, NASA
HAMPTON, VIRGINIA

October 1984

NASA

INCOMPRESSIBLE LIFTING-SURFACE AERODYNAMICS FOR A ROTOR-STATOR COMBINATION

Sridhar M. Ramachandra*
National Aeronautics and Space Administration
Lewis Research Center
Cleveland, Ohio 44135

SUMMARY

Current literature on the three-dimensional flow through compressor cascades deals with a row of rotor blades in isolation. Since the distance between the rotor and stator is usually 10 to 20 percent of the blade chord, the aerodynamic interference between them has to be considered for a proper evaluation of the aerothermodynamic performance of the stage. A unified approach to the aerodynamics of the incompressible flow through a stage is presented that uses the lifting-surface theory for a compressor cascade of arbitrary camber and thickness distribution. The effects of rotor-stator interference are represented as a linear function of the rotor and stator flows separately. The loading distribution on the rotor and stator blades and the interference factor are determined concurrently through a matrix iteration process.

INTRODUCTION

The multistage axial compressor functions in such a way that each stage performs essentially the same basic function as the other. Air from the rotor enters the stator, which is placed close behind it, usually within a distance of 10 to 20 percent of the blade chord. The rotor imparts kinetic energy of rotation to the basically axial incoming free-stream flow and also increases its potential energy in the form of a static pressure rise while passing through the interblade passages. The stator converts the kinetic energy of rotation of the entering air into potential energy by a further increase of the static pressure so that the flow downstream of the stator is, again, nearly axial.

Current literature on the three-dimensional flow in turbomachines is concerned mainly with the flow over one row of rotor blades in isolation. In the single actuator disk model the perturbation velocity of the disk decreases exponentially with the distance from the disk. Qualitatively, the strong upwash field of the stator blades affects a substantial portion of the flow over the rotor blades and in turn increases the effective incidence of the rotor blades. Thus the rotor blades are closer to positive stall with the stator than without, when the effective incidence of the rotor blades is high in a positive sense. Similarly, when the effective incidence of the stator blades is high in a negative sense, the stator blades are closer to negative stall with the rotor than without.

Thus it is important to consider the combination of the two rows, which form one stage of an axial turbomachine, in order to understand their interference effects and obtain a more accurate evaluation of the dynamic and

*NRC-NASA Resident Research Associate.

aerothermodynamic behavior of the multistage compressor as a system through a synthesis of the individual stage performances.

Actuator disk models of the multistage compressor basically assume each blade row to be of zero axial thickness. In these models such an arrangement of many stages is equivalent to flow through a series of thin actuator disks. Using the actuator disk model, Traupel (ref. 1) dealt with the case of an axially symmetric, multistage machine with an infinite number of identical equidistant stages. He introduced an axially periodic stream function, with a period of one stage pitch, to describe the flow and obtained an expression for the radial velocity.

Marble (ref. 2), Marble and Michelson (ref. 3), and Raily (ref. 4) considered extensions of the actuator disk concept to disks of nonzero axial thickness. Thus Marble considered an axially symmetric flow through an actuator disk with the vorticity shed from each blade row distributed continuously over the region behind the blade. He obtained a linear equation for the radial velocity on each side of the disk and obtained a solution for a blade row of finite chord by superposition.

Raily (ref. 4) assumed the radial velocity field in the multistage compressor to be the sum of the radial velocity contribution of each stage in isolation and the axial and whirl velocities to remain the same for each blade row. He assumed an exponential variation of the radial velocity components along the axis and determined the radial variation. Assuming an initial axial velocity for each stage, Raily calculated the radial velocity fields by superposition of the stage contributions and used these fields to recalculate the axial velocities iteratively in order to obtain the final solution. He also calculated the whirl components for each case from the velocity triangles.

Horlock (ref. 5) used the actuator disk model to study the effect of locating the actuator disk in the plane of the blade trailing edge and in the plane of the center of pressure of each blade row. Horlock and Deverson (ref. 6) found that theory and experiment agreed best for placement of the actuator disk at the midaxial plane of the blades.

Kemp and Sears (refs. 7 and 8) studied the aerodynamic interference between the rotor and stator-blade rows for incompressible, nonviscous fluids by regarding each blade row as an infinite two-dimensional cascade. They obtained expressions for the unsteady components of lift and moment of the blades of each row. They also calculated the effects of stator wakes on the unsteady lift of rotor blades. They found lift fluctuation amplitudes of about 18 percent of the steady lift. Besides, viscous interaction on the forces and moments caused unsteady forces and moments of about the same order as the aerodynamic interference between the blade rows.

Prandtl and Betz (ref. 9) outlined the lifting-line theory of the propeller for minimum energy losses in an incompressible inviscid fluid. This theory was followed by Goldstein (ref. 10), who formulated the incompressible potential vortex theory of a propeller with a bound vortex line for each blade and a helical trailing vortex sheet shed from its trailing edge. This theory was improved and later extended to linearized compressible potential flow for the propeller by Busemann (ref. 11) and Davidson (ref. 12) and to the flow through a compressor by Rott (ref. 13).

A linearized three-dimensional lifting-line theory for an axial compressor blade row in an infinite axial duct was proposed by McCune (refs. 14 and 15) and by McCune and Okorounmu (ref. 16) for both subsonic and supersonic flow. However, McCune's results are applicable to nonlifting blades. Later, Namba (ref. 17) proposed the lifting-surface theory for a rotating thin blade row for subsonic and supersonic Mach numbers that uses a distribution of oscillating pressure dipoles on the blades. His theory does not consider the effects of blade thickness, camber, and incidence. The effects of trailing vortices shed by the blades are omitted since he used the acceleration potential. Furthermore, Namba's theory does not consider the radial velocity or the swirl velocity component at the inlet other than the circumferential velocity due to blade rotation.

Wu (ref. 18) proposed a linearized, three-dimensional, compressible fluid flow for axial-, radial-, and mixed-flow turbomachines and outlined a numerical solution technique for the differential equations.

The present report deals with the direct turbomachine problem by considering the rotationally symmetric, three-dimensional, steady, incompressible ideal fluid flow through an axial compressor stage consisting of a finite number of blades in the rotor and stator. The rotor and stator are assumed to be located centrally in an infinite, coaxial, cylindrical duct with only a small clearance between the blade tips and the duct walls.

The stator experiences a periodic flow when cutting through the multiple-start helical vortex sheets of the rotor wake. For simplicity, it is assumed that the discrete multiple-start, helical, trailing vortex sheets may be replaced by an equivalent continuous vortex cylinder of the same root and tip diameter but with uniform vorticity over its cross section. In this representation the stator blades will experience a steady incoming flow. The effect of nonuniform/discontinuous wake vorticity is considered separately.

In the present study both the rotor and the stator blades are considered to be straight, rigid, and untapered. The incoming flow into the rotor is assumed to be uniform and axial with no radial or swirl component other than that due to the rotor rotation. Furthermore the inflow into the stator is assumed to be primarily a uniform axial velocity with a varying swirl component imparted by the rotor. The radial inlet velocity component due to the rotor is neglected at this stage.

The undisturbed free-stream velocity components are taken to be $(0, V_r, W_r)$ in the (r, θ, Z) directions relative to the rotor in a cylindrical coordinate system. The air is assumed to enter the rotor with uniform upstream static pressure p_∞ and density ρ_∞ and with an axial velocity W_r that is uniformly distributed over the rotor face.

To simplify the mathematical treatment and the application of surface boundary conditions, the stator is considered to be stationary. For the stator the radial velocity component in the rotor outflow is neglected as negligible so that the inlet velocity components for the stator are assumed to be $0, V_s,$ and W_s . Since the stator is situated close to the rotor exit in a region of rapid change, it is not possible to define, a priori, the inlet velocity components $0, V_s,$ and W_s exactly. However, the stator inlet conditions are assumed to correspond approximately to the value obtained from the velocity vector diagram (fig. 1) so that the inlet velocity to the stator would have

the components 0 , $V_r - W_r \tan \alpha_2$, and W_r . Assuming that the rotor and stator are lightly loaded, this is tantamount to the hypothesis that the perturbation velocity components due to the rotor are small as compared with components given at this stage, that the stator axial velocity W_s is uniform and equals W_r , and that the circumferential velocity V_s is uniform and equals $V_r - W_r \tan \alpha_2$.

In the following sections a scheme for representing the lifting-surface of rotor and stator blades of arbitrary geometry through a distribution of flow singularities is discussed, and their induced velocity fields at an arbitrary point of the flow are obtained. The rotor-stator interference factor is introduced next, and matching of the resultant flow field of the stage to provide zero net vorticity downstream of the stage is discussed. The boundary conditions on the blade surfaces are given in terms of blade and cascade geometry. These are reduced to a set of simultaneous algebraic equations to determine both the set of constants giving the distribution of flow singularities and the interaction factor. The problem is then discretized, and an iterative scheme for the solution of the matrix of unknown constants is outlined. The net pressure distribution on the blades is expressed in terms of the induced velocities, and applications are briefly discussed.

SYMBOLS

A_m	expansion coefficients for rotor-blade chordwise vorticity distribution (eq. (11a))
\hat{A}_m	modified rotor chordwise vorticity distribution coefficients (eq. (27))
\mathcal{A}	matrix of coefficients \hat{A}_m (eq. (61))
AA	column vector of constants \hat{A}_m , \hat{B}_m , \hat{C}_m , \hat{D}_m , and ϵ_1
B_m	expansion constants for rotor-blade chordwise source distribution (eq. (11c))
\hat{B}_m	modified rotor-blade chordwise source distribution coefficients (eq. (27))
\mathcal{B}	matrix of coefficients \hat{B}_m (eq. (61))
C_m	expansion constants for stator-blade chordwise vorticity distribution (eq. (11b))
\hat{C}_m	modified stator chordwise vorticity distribution coefficients (eq. (27))
C_R, C_S	rotor- and stator-blade half-chord lengths
C^*	dimensionless rotor- and stator-blade half-chords
\mathcal{C}	matrix of coefficients (eq. (61))

c_{lr}, c_{ls}	local lift coefficient of rotor and stator blades
D_m	expansion coefficients for stator-blade chordwise source distribution (eq. (11d))
\hat{D}_m	modified stator-blade chordwise source distribution coefficients (eq. (27))
\mathcal{D}	matrix of coefficients (eq. (61))
E_{rm}, E_{sm}	rotor and stator functions (eq. (35))
EE	matrix defined in (eq. (59))
EF	matrix of integrals (eq. (57))
EM_i	matrix elements defined in eq. (60) ($i = 1, 2, 3, 4$)
\vec{F}_m	vector integral defined in eqs. (28a) and (52)
\mathcal{F}_m	matrix defined in (eq. (50))
\vec{G}_m	vector integral defined in eqs. (28b) and (52)
\mathcal{G}_m	matrix defined in eq. (50)
g_r, g_s	rotor and stator geometry functions (eq. (49))
\vec{H}_m	vector integral defined in eqs. (28c) and (52)
\mathcal{H}_m	matrix defined in eq. (50)
h_r, h_s	rotor and stator (hub/tip) radius ratio
\vec{J}_m	vector integral defined in eqs. (28d) and (52)
\mathcal{J}_m	matrix defined in eq. (50)
k_r, k_s	rotor and stator circumferential mode numbers
L_r, L_s	lift per unit span of rotor and stator blades
M	Mach number
M_*	matrix dimension parameter, $R \times N_*$
N_*	number of chordwise stations on blade
p_∞	free-stream static pressure
p_r, p_s	perturbation pressures due to rotor and stator
p_{or}, p_{os}	total pressures ahead of rotor and stator

$\Delta P_r, \Delta P_s$	net pressure difference on rotor and stator blades (eq. (68))
Q_r	total source density on rotor blade (eq. (11))
Q_s	total source density on stator-blade (eq. (11))
R_r, R_s	functions defined in eq. (30)
R_{sr}	ratio of stator tip radius to rotor tip radius, r_{ts}/r_{tr}
R_*	number of stations along blade radius
$\vec{r}(r, \theta, z)(x, y, z)$	position vector of arbitrary point (cylindrical/Cartesian coordinates)
r_l	dimensionless radial coordinate, r/r_{tr}
r_{hr}, r_{hs}	hub radius of rotor and stator
r_{tr}, r_{ts}	tip radius of rotor and stator
S_{rh}, S_{sh}	functions defined at rotor and stator hub (eq. (36))
SR	matrix defined in eq. (51)
T_{rm}, T_{sm}	rotor and stator functions defined in eq. (47)
\vec{U}_R, \vec{U}_S	resultant total velocity of rotor and stator
$\vec{\hat{U}}_R, \vec{\hat{U}}_S$	modified resultant total velocity of rotor and stator (eq. (39))
\vec{U}	resultant induced velocity vector (eq. (25))
$\vec{\hat{U}}$	modified resultant induced velocity (eqs. (26) and (27)), \vec{U}/W_a
V_r, V_s	circumferential velocity of air for rotor and stator
\vec{V}_r, \vec{V}_s	free-stream velocity vector for rotor and stator
$\vec{\hat{V}}_r, \vec{\hat{V}}_s$	modified free-stream velocity vector for rotor and stator (eq. (39))
W_r, W_s	axial velocity of air for rotor and stator
(x, y, z)	Cartesian coordinates of arbitrary point
$(y'_r, z'_r), (y'_s, z'_s)$	Cartesian coordinates of rotor and stator in local coordinate system of blade

z_r, z_s	number of blades in rotor and stator
$\mathcal{Z}_{1r}, \mathcal{Z}_{2r}$	rotor vector function (eq. (29))
$\mathcal{Z}_{1s}, \mathcal{Z}_{2s}$	stator vector function (eq. (29))
z_{Cr}^i, z_{Cs}^i	mean-line ordinate of rotor- and stator-blade profiles
z_{Lr}^i, z_{Ls}^i	lower surface ordinate of rotor- and stator-blade profiles
z_{Tr}^i, z_{Ts}^i	local half-thickness of rotor- and stator-blade profiles
z_{Ur}^i, z_{Us}^i	upper surface ordinate of rotor- and stator-blade profiles
z_{r0}, z_{s0}	axial position of midrotor and midstator plane from reference origin
z_{r1}, z_{r2}	axial coordinate of stator-blade leading and trailing edges
z_{s1}, z_{s2}	axial coordinate of stator-blade leading and trailing edges
α_r, α_s	blade angle settings of rotor and stator blades
α_{2r}	exit blade angle of rotor
Γ_r, Γ_s	total vorticity density of rotor and stator blades (eq. (11))
ϵ	rotor-stator interaction factor
ϵ_1	interaction parameter (eq. (56)), $1/(1 + \epsilon)$
θ	azimuth angle of cylindrical coordinate system
$\lambda_{\ell}^{(k_r)}, \lambda_{\ell}^{(k_s)}$	ℓ -th eigenvalue for mode m_r, m_s
ν_r, ν_s	mean azimuth angle of m_r -th rotor blade, m_s -th stator blade (eq. (14))
$\vec{P}(\rho, \psi, \zeta)$	position vector of a point on rotor/stator with cylindrical coordinates ρ, ψ, ζ
ρ_r, ρ_s	radial position of source/vortex on rotor and stator blades
$\Phi_{\ell}^{(k_r)}$	normalized Bessel function of rotor blade of mode number k_r and ℓ -th eigenvalue
φ_r, φ_s	azimuth angle of source/vortex on rotor and stator blades

$\bar{\varphi}_r, \bar{\varphi}_s$	mean offset angle of first rotor and stator blades
$\Psi^{(k_s)}$	normalized Bessel function of stator blade of mode number k_s and l -th eigenvalue
ψ_r, ψ_s	azimuth angle of point on m_r -th rotor and stator blades defined in eqs. (12) and (18)
Ω	angular velocity of rotor
ω_r, ω_s	Glauert angle of blade defined in eq. (1)
Subscripts:	
r, s	rotor, stator
h, t	hub, tip
i, j, k	unit vectors along (x, y, z) directions

REPRESENTATION OF LIFTING SURFACE

The blades of the stage are considered to be thin with small camber. The pressure distribution on the blade may be regarded as arising from a surface distribution of flow singularities that give rise to the given blade profile and its lift. The thickness effect of the blade is represented by a surface distribution of sources and its lift distribution by a surface distribution of vortices. The distribution of both the source and vortex singularities varies radially and chordwise over the blade section. A study of the linearized partial differential equations for the perturbation pressures of the rotor and stator when the fluid is incompressible shows that the radial variation of the pressure satisfies Bessel's differential equation. Therefore, to provide for the radial variation of the singularities, the chordwise variation is modulated by a Bessel function.

To specify the chordwise distribution, it is convenient to refer to a locally rotated coordinate system ($Y'_r - Z'_r$) (fig. 2) and to define the Glauert angles ω_r and ω_s , for a point on the rotor- and stator-blade chords, respectively, through the equations

$$\left. \begin{aligned} y'_r &= -C_R \cos \omega_r; & -C_R \leq y'_r \leq C_R; & & 0 \leq \omega_r \leq \pi \\ y'_s &= C_S \cos \omega_s; & -C_S \leq y'_s \leq C_S; & & 0 \leq \omega_s \leq \pi \end{aligned} \right\} \quad (1)$$

If the midpoint of the blade chord is used as the reference origin for each blade, the unit vectors in the (R, Y', Z') coordinate system are related to the unit vectors (R, θ, Z) in the cylindrical coordinates by the transformation

$$\begin{pmatrix} R \\ Y'_r \\ Z'_r \end{pmatrix} = \begin{pmatrix} 1 & 0 & 0 \\ 0 & \sin \alpha_r & \cos \alpha_r \\ 0 & -\cos \alpha_r & \sin \alpha_r \end{pmatrix} \begin{pmatrix} R \\ \theta \\ Z \end{pmatrix} \quad (2a)$$

$$\begin{pmatrix} R \\ Y'_s \\ Z'_s \end{pmatrix} = \begin{pmatrix} 1 & 0 & 0 \\ 0 & \sin \alpha_s & \cos \alpha_s \\ 0 & -\cos \alpha_s & \sin \alpha_s \end{pmatrix} \begin{pmatrix} R \\ \theta \\ Z \end{pmatrix} \quad (2b)$$

This system of coordinates is rotated from the plane of rotation by the angles α_r and α_s , respectively. The relation between the coordinates (Y'_r, Z'_r) and (Y'_s, Z'_s) of a point on a rotor or stator blade with the corresponding coordinates (Y_r, Z_r) and (Y_s, Z_s) in the $(Y - Z)$ system is given by the equations

$$\begin{pmatrix} R \\ Y'_r \\ Z'_r \end{pmatrix} = \begin{pmatrix} \cos \psi_r & \sin \psi_r & 0 \\ -\sin \alpha_r \sin \psi_r & \sin \alpha_r \cos \psi_r & \cos \alpha_r \\ \cos \alpha_r \sin \psi_r & -\cos \alpha_r \cos \psi_r & \sin \alpha_r \end{pmatrix} \begin{pmatrix} X_r \\ Y_r \\ Z_r \end{pmatrix} \quad (3)$$

$$\begin{pmatrix} R \\ Y'_s \\ Z'_s \end{pmatrix} = \begin{pmatrix} \cos \psi_s & \sin \psi_s & 0 \\ -\sin \alpha_s \sin \psi_s & \sin \alpha_s \cos \psi_s & \cos \alpha_s \\ \cos \alpha_s \sin \psi_s & -\cos \alpha_s \cos \psi_s & \sin \alpha_s \end{pmatrix} \begin{pmatrix} X_s \\ Y_s \\ Z_s \end{pmatrix} \quad (4)$$

where

$$\left. \begin{aligned} z_{r1} &= z_{r0} - C_R \cos \alpha_r; & z_{r2} &= z_{r0} + C_R \cos \alpha_r \\ z_{s1} &= z_{s0} - C_S \cos \alpha_s; & z_{s2} &= z_{s0} + C_S \cos \alpha_s \end{aligned} \right\} \quad (5)$$

and (z_{r1}, z_{r2}) and (z_{s1}, z_{s2}) refer to the leading and trailing edges of the rotor and stator. The cylindrical coordinates of an arbitrary point y_r, y_s on the rotor- and stator-blade chord at any radius r are given by

$$\left. \begin{aligned} r_1; & \quad \bar{\varphi}_r + \nu_r - \arctan \frac{C_R}{r_1} \cos \omega_r \sin \alpha_r; & z_{r0} + C_R \cos \omega_r \cos \alpha_r \\ r_1; & \quad \varphi_s + \nu_s - \arctan \frac{C_S}{r_1} \cos \omega_s \sin \alpha_s; & z_{s0} + C_S \cos \omega_s \cos \alpha_s \\ & -1 \leq y'_r, y'_s \leq +1; & h_r \leq r \leq 1; & h_s R_{sr} \leq r \leq R_{sr} \end{aligned} \right\} \quad (6)$$

Note that the chordwise coordinates y'_r and y'_s are normalized relative to the chords $2C_R$ and $2C_S$, respectively.

If z'_{Cr} and z'_{Cs} refer to the mean camber line of the rotor- and stator-blade profiles and z'_{Tr} and z'_{Ts} refer to the half-thickness of the corresponding blades, we have the relations

$$\left. \begin{aligned} z_{Cr}^i &= z_{Cr}^i(y_r^i); & z_{Tr}^i &= z_{Tr}^i(y_r^i) \\ z_{Cs}^i &= z_{Cs}^i(y_s^i); & z_{Ts}^i &= z_{Ts}^i(y_s^i) \end{aligned} \right\} \quad (7)$$

The equation of the upper and lower surface blade profiles can be obtained from

$$\begin{aligned} z_{Ur}^i &= z_{Cr}^i + z_{Tr}^i; & z_{Lr}^i &= z_{Cr}^i - z_{Tr}^i \\ z_{Us}^i &= z_{Cs}^i + z_{Ts}^i; & z_{Ls}^i &= z_{Cs}^i - z_{Ts}^i \end{aligned} \quad (8)$$

Following Schlichting (ref. 19), the chordwise distribution of the flow singularities is assumed to have the form of a Glauert-Birnbaum series (refs. 20 and 21). Furthermore because of the three-dimensional nature of the flow, the Glauert expansion will be modulated by suitable functions Φ_* and Ψ_* of the radius. These functions are obtained as sums of the eigenfunctions

$\Phi_{\ell}^{(k_r)}$, $\Psi_{\ell}^{(k_s)}$. In turn, $\Phi_{\ell}^{(k_r)}$ and $\Psi_{\ell}^{(k_s)}$ are normalized linear combinations of Bessel and Neumann functions of order k_r and k_s for the ℓ -th eigenvalue $\lambda_{\ell}^{(k_r)}$ and $\lambda_{\ell}^{(k_s)}$ of the rotor and stator

The functions $\Phi_{\ell}^{(k_r)}$ and $\Psi_{\ell}^{(k_s)}$ are normalized linear combinations of Bessel and Neumann functions of order k_r and k_s for the ℓ -th eigenvalue for the rotor and stator and can be written

$$\left. \begin{aligned} \Phi_{\ell}^{(k)} &= \left[\frac{Y^{(k-1)}(\lambda_{\ell}^{(k)} h_r) - Y^{(k+1)}(\lambda_{\ell}^{(k)} h_r)}{J^{(k-1)}(\lambda_{\ell}^{(k)} h_r) - J^{(k+1)}(\lambda_{\ell}^{(k)} h_r)} \right] \\ &\quad \times J^{(k)}(r_1 \lambda_{\ell}^{(k)}) + Y^{(k)}(r_1 \lambda_{\ell}^{(k)}) \\ \Psi_{\ell}^{(k)} &= \left[\frac{Y^{(k-1)}(\lambda_{\ell}^{(k)} R_{sr} h_s) - Y^{(k+1)}(\lambda_{\ell}^{(k)} R_{sr} h_s)}{J^{(k-1)}(\lambda_{\ell}^{(k)} R_{sr} h_s) - J^{(k+1)}(\lambda_{\ell}^{(k)} R_{sr} h_s)} \right] \\ &\quad \times J^{(k)}(\lambda_{\ell}^{(k)} r_1) + Y^{(k)}(\lambda_{\ell}^{(k)} r_1) \end{aligned} \right\} \quad (9)$$

The pressure eigenfunctions $\Phi_{\ell}^{(k_r)}$ and $\Psi_{\ell}^{(k_s)}$ satisfy the end conditions at the root and tip expressed by the equations

$$\left. \begin{aligned} \frac{d}{dr_1} \Phi_{\ell}^{(k)}(r_1) &= 0 & \text{at } r_1 = h_r \text{ and } r_1 = 1 \\ \frac{d}{dr} \Psi_{\ell}^{(k)}(r_1) &= 0 & \text{at } r_1 = h_s R_{sr} \text{ and } r_1 = R_{sr} \end{aligned} \right\} \quad (10)$$

which represent zero radial velocity corresponding to zero radial pressure gradient at the hub and tip of the rotor and stator. The eigenvalues

$\lambda_{\ell}^{(k)}$ for the rotor and stator are given by the roots of the corresponding transcendental equations obtained by satisfying the end conditions (eq. (10)) at the blade tip.

Although the inlet flow conditions for the stator are really periodic as a result of the perturbations introduced by the rotor blade passing each point with a frequency $\bar{\omega}_s = Z_r \Omega / 2\pi$, in this paper, it is simply assumed that the stator-blade inlet conditions are steady by putting $\bar{\omega}_s = 0$.

The total surface density of source and vorticity for the complete range of eigenvalues ($\ell = 0, 1, 2, \dots, \infty$) and the mode numbers k_r and k_s ($k_r, k_s = 0, \pm 1, \pm 2, \dots, \pm \infty$) is given by

$$\Gamma_r(\vec{\rho}_r) = 2W_a \left(A_0 \cot \frac{\omega_r}{2} + \sum_{m=1}^{\infty} A_m \sin m\omega_r \right) \Phi_*(\rho_r) \quad (11a)$$

$$\Gamma_s(\vec{\rho}_s) = 2W_a \left(C_0 \cot \frac{\omega_s}{2} + \sum_{m=1}^{\infty} C_m \sin m\omega_s \right) \Psi_*(\rho_s) \quad (11b)$$

$$Q_r(\vec{\rho}_r) = 2W_a \left[B_0 \left(\cot \frac{\omega_r}{2} - 2 \sin \omega_r \right) + \sum_{m=2}^{\infty} B_m \sin m\omega_r \right] \Phi_*(\rho_r) \quad (11c)$$

$$Q_s(\vec{\rho}_s) = 2W_a \left[D_0 \left(\cot \frac{\omega_s}{2} - 2 \sin \omega_s \right) + \sum_{m=2}^{\infty} D_m \sin m\omega_s \right] \Psi_*(\rho_s) \quad (11d)$$

$$\Phi_*(\rho_r) = \sum_{k_r=-\infty}^{\infty} \sum_{\ell=0}^{\infty} D_{\ell}^{(k_r)}(\rho_r) \quad \Psi_*(\rho_s) = \sum_{k_s=-\infty}^{\infty} \sum_{\ell=0}^{\infty} \Psi_{\ell}^{(k_r)}(\rho_s)$$

The expansion coefficients A_m, B_m, C_m , and D_m ($m = 0, 1, 2, \dots, \infty$) are determined by satisfying the boundary conditions on the rotor and stator blades simultaneously. The cylindrical coordinates $(\rho_r, \psi_r, \zeta_r)$ and $(\rho_s, \psi_s, \zeta_s)$ of a point on the m_r -th rotor blade and m_s -th stator blade are related to the corresponding chordwise coordinates (ω_r, ρ_r) and (ω_s, ρ_s) the relations

$$\left. \begin{aligned}
\psi_r &= \bar{\varphi}_r + \left(\frac{2\pi m_r}{Z_r} \right) - \arctan \left(\frac{C_R \sin \alpha_r \cos \omega_r}{\rho_r} \right) \\
\psi_s &= \bar{\varphi}_s + \left(\frac{2\pi m_s}{Z_s} \right) + \arctan \left(\frac{C_S \sin \alpha_s \cos \omega_s}{\rho_s} \right) \\
\zeta_r &= z_{r0} + C_R \cos \alpha_r \cos \omega_r \\
\zeta_s &= z_{s0} - C_S \cos \alpha_s \cos \omega_s
\end{aligned} \right\} \quad (12)$$

The distributions assumed in equations (2), (3), or (9) for the flow singularities are such that the vorticity density $\Gamma(\rho, \varphi, \zeta)$ becomes infinite at the blade leading edge ($\omega = 0$) to give infinite suction and vanishes at the trailing edge ($\omega = \pi$), satisfying the Kutta condition as in the case of a flat plate at incidence for both the rotor and the stator. The assumed source density $Q(\rho, \varphi, \zeta)$ vanishes at the trailing edge ($\omega = \pi$) and becomes infinite at the leading edge ($\omega = 0$), corresponding to the case of symmetric Joukowski profile at zero incidence.

Induced Velocity Field of Bound Vorticity

Assuming that the bound vortex filaments have their axes along radial lines and considering a rotor-blade surface area element ($d\rho_r d\zeta_r \sec \alpha_r$), the vorticity contained in the element is $\Gamma_r(\rho_r, \varphi_r, \zeta_r) \sec \alpha_r d\rho_r d\zeta_r$. The induced velocity $d\vec{u}_r$, at the point (r, θ, z) in the flow field, due to the bound vortex filament with a unit vector \vec{M}_r at $\vec{\rho}_r(\rho_r, \varphi_r, \zeta_r)$ can be obtained from Biot-Savart's law as

$$d\vec{u}_r = \Gamma_r(\rho_r, \varphi_r, \zeta_r) \sec \alpha_r \vec{M}_r \times \frac{(\vec{r} - \vec{\rho}_r)}{4\pi |\vec{r} - \vec{\rho}_r|^3} d\rho_r d\zeta_r \quad (13)$$

which can be written as

$$d\vec{u}_r = \{ -\vec{i}(z - \zeta_r) \sin \psi_r + \vec{j}(z - \zeta_r) \cos \psi_r - \vec{k}r \sin(\theta - \psi_r) \} \\
\times \left[\frac{\Gamma_r(\rho_r, \psi_r, \zeta_r) \sec \alpha_r}{4\pi R_r^3(\vec{r}_1, \vec{\rho}_r)} d\rho_r d\zeta_r \right] \quad (14)$$

where \vec{i} , \vec{j} , and \vec{k} are the unit vectors along the (x, y, z) directions and the angle ψ_r is defined by

$$\psi_r = \bar{\varphi}_r + \varphi_r + v_r \quad v_r = 2\pi m_r / Z_r; \quad m_r = 0, 1, 2, \dots, (Z_r - 1) \quad (15)$$

The induced velocity $d\vec{u}_r$ due to all of the Z_r blades and all of the circumferential orders k_r at the blade element is given by

$$4\pi \cos \alpha_r d\vec{u}_r = \sum_{m_r=0}^{Z_r-1} \left[-\vec{i}(z - \zeta_r) \sin \psi_r + \vec{j}(z - \zeta_r) \cos \psi_r - \vec{k}r \sin (\theta - \psi_r) \right] \\ \times \left[\frac{\Gamma_r(\rho_r, \psi_r, \zeta_r)}{R_r^3(\vec{r}_1, \vec{\rho}_r)} \right] d\rho_r d\zeta_r$$

Introducing the vorticity distribution from equation (2a) into equation (15) and integrating with respect to ρ_r and ζ_r gives the induced velocity \vec{u}_r due to the vorticity on the whole blade surface.

$$\frac{2\pi \cos \alpha_r \vec{u}_{r\Gamma}}{W_a} = \int_{h_r}^1 \int_{z_{r1}}^{z_{r2}} \sum_{m_r=0}^{Z_r-1} \sum_{k_r=-\infty}^{\infty} [-\vec{i}(z_1 - \zeta_r) \sin c_r + \vec{j}(z - \zeta_r) \\ \times \cos \psi_r - \vec{k}r \sin (\theta - \psi_r)] \left(A_0 \cot \frac{\omega_r}{2} + \sum_{m=1}^{\infty} A_m \sin m\omega_r \right) \\ \times \Phi_*(\rho_r) R_r^{-3}(\vec{r}_1, \vec{\rho}_r) d\zeta_r d\rho_r \quad (17)$$

Similarly, by defining ψ_s and v_s by

$$\left. \begin{aligned} \psi_s &= \bar{\varphi}_s + \varphi_s + v_s \\ v_s &= \frac{2\pi m_s}{Z_s} \end{aligned} \right\} m_s = 0, 1, 2, \dots, m(Z_s - 1) \quad (18)$$

We can write the induced velocity due to the bound vorticity on the stator blades as

$$\frac{2\pi \cos \alpha_s \vec{u}_{s\Gamma}}{W_a} = \int_{R_{sr}h_s}^{R_{sr}} \int_{z_{s1}}^{z_{s2}} \sum_{k_s=-\infty}^{\infty} \sum_{m_s=0}^{Z_s-1} [-\vec{i}(z_1 - \zeta_s) \sin \psi_s + \vec{j}(z_1 - \zeta_s) \\ \times \cos \psi_s - \vec{k}r \sin (\theta - \psi_s)] \left(C_0 \cot \frac{\omega_s}{2} + \sum_{m=1}^{\infty} C_m \sin m\omega_s \right) \\ \times \Psi_*(\rho_s) R_s^{-3}(\vec{r}_1, \vec{\rho}_s) d\zeta_s d\rho_s \quad (19)$$

Induced Velocity Field of Source Distribution

For a rotor-blade surface-area element ($d\rho_r d\zeta_r \sec \alpha_r$), the source of strength $Q_r(\rho_r, \psi_r, \zeta_r) \sec \alpha_r d\rho_r d\zeta_r$ at $(\rho_r, \psi_r, \zeta_r)$ induces

a velocity $d\vec{u}_r(u_r', v_r', w_r')$ at the point (r_1, θ, z) in the flow. The velocity is obtained from Biot-Savart's law as

$$d\vec{u}_r = Q_r(\rho_r, \psi_r, \zeta_r) \sec \alpha_r \frac{\vec{r}_1 - \vec{\rho}_r}{4\pi R_r^3(r_1, \rho_r)} d\rho_r d\zeta_r \quad (20)$$

whose Cartesian components can be obtained from the expression

$$4\pi \cos \alpha_r d\vec{u}_r = [(r_1 \cos \theta - \rho_r \cos \psi_r)\vec{i} + (r_1 \sin \theta - \rho_r \sin \psi_r)\vec{j} + (z - \zeta_r)\vec{k}] \times \left[\frac{Q_r(\rho_r, \psi_r, \zeta_r)}{R_r^3(\vec{r}_1, \vec{\rho}_r)} \right] d\rho_r d\zeta_r \quad (21)$$

The induced velocity $d\vec{u}_r$ due to the sources on all of the Z_r blades located at the same relative location for the whole set of circumferential orders k_r is given by the summation

$$4\pi \cos \alpha_r d\vec{u}_r = \sum_{m_r=0}^{Z_r-1} \left[\frac{\vec{i}(r_1 \cos \theta - \rho_r \cos \psi_r) + \vec{j}(r_1 \sin \theta - \rho_r \sin \psi_r) + \vec{k}(z_1 - \zeta_r)}{R_r(\vec{r}_1, \vec{\rho}_r)^3} \right] \times Q_r(\rho_r, \psi_r, \zeta_r) d\rho_r d\zeta_r \quad (22)$$

Again, by introducing the source distribution from equation (11c) into equation (22), the induced velocity \vec{u}_r due to the source distribution over the whole rotor-blade surface can be obtained by integrating with respect to ρ_r and ζ_r and is given by

$$\left(\frac{2\pi \cos \alpha_r}{W_a} \right) \vec{u}_{rQ} = \int_{h_r}^1 \int_{z_{r1}}^{z_{r2}} \sum_{m_r=0}^{Z_r-1} \left[\vec{i}(r_1 \cos \theta - \rho_r \cos \psi_r) + \vec{j}(r_1 \sin \theta - \rho_r \sin \psi_r) + \vec{k}(z_1 - \zeta_r) \right] \left[B_0 \left(\cot \frac{\omega_r}{2} - 2 \sin \omega_r \right) + \sum_{m=2}^{\infty} B_m \sin m\omega_r \right] \times \rho_r R_r^{-3}(\vec{r}_1, \vec{\rho}_r) d\rho_r d\zeta_r \quad (23)$$

Similarly, the induced velocity due to the source distribution on the Z_s stator blades can be written for the whole set of circumferential orders k_s as

$$\begin{aligned}
\left(\frac{2\pi \cos \alpha_s}{W_a} \right) \vec{u}_{sQ} = & \int_{R_{sr} h_s}^{R_{sr}} \int_{z_{s1}}^{z_{s2}} \sum_{m_s=0}^{Z_s-1} \left[\vec{i}(r_1 \cos \theta - \rho_s \cos \psi_s) + \vec{j}(r \sin \theta \right. \\
& \left. - \rho_s \sin \psi_s) + \vec{k}(z_1 - \zeta_s) \right] \left[D_0 \cot \frac{\omega_s}{2} - 2 \sin \omega_s + \sum_{m=2}^{\infty} D_m \sin m\omega_s \right] \\
& \times \Psi_{\rho_s} R_s^{-3} (\vec{r}_1, \vec{\rho}_s) d\rho_s d\zeta_s
\end{aligned} \quad (24)$$

Induced Velocity of Combined Source and Vortex System of Rotor and Stator

For low subsonic axial flow ($M \ll 1$) the resultant induced velocity $\vec{u}(\vec{r})$ at an arbitrary point $\vec{r}(r, \theta, z)$ of the flow field due to the combined system of sources and vortices on both the rotor and stator is obtained from the equation

$$\vec{u} = \vec{u}_{r\Gamma} + \vec{u}_{s\Gamma} + \vec{u}_{rQ} + \vec{u}_{sQ} \quad (25)$$

By combining equations (16), (18), (23), and (24), \vec{u} can be expressed in terms of the expansion coefficients of the Glauert series of equations (2) as

$$\vec{u} = \sum_{m=0}^{\infty} (\hat{A}_m \vec{F}_m + \hat{B}_m \vec{G}_m + \hat{C}_m \vec{H}_m + \hat{D}_m \vec{J}_m) \quad (26)$$

where \hat{u} , \hat{A}_m , \hat{B}_m , \hat{C}_m , and \hat{D}_m are redefined by the coefficients

$$\begin{aligned}
\hat{A}_m &= A_m / \cos \alpha_r & \hat{B}_m &= B_m / \cos \alpha_r & \hat{\vec{u}} &= \vec{u} / W_a \\
\hat{C}_m &= C_m / \cos \alpha_s & \hat{D}_m &= D_m / \cos \alpha_s & \hat{Q} &= Q / 2W_a
\end{aligned}$$

and \vec{F}_m , \vec{G}_m , \vec{H}_m , and \vec{J}_m are the set of vector functions defined for the rotor and stator by

$$2\pi \begin{pmatrix} \vec{F}_0 \\ \equiv \\ \vec{F}_m \end{pmatrix} = \int_{h_r}^1 \int_{z_{r1}}^{z_{r2}} \vec{\mathcal{F}}_{1r}(\vec{r}_1, \vec{\rho}_r) \begin{pmatrix} \cot \frac{\omega_r}{2} \\ \equiv \\ \sin m\omega_r \end{pmatrix} \Phi(\rho_r) d\rho_r d\zeta_r \quad (28a)$$

$$2\pi \begin{pmatrix} \vec{G}_0 \\ \equiv \\ \vec{G}_m \end{pmatrix} = \int_{h_r}^1 \int_{z_{r1}}^{z_{r2}} \vec{\mathcal{F}}_{2r}(\vec{r}_1, \vec{\rho}_r) \begin{pmatrix} \cot \frac{\omega_r}{2} \\ \equiv \\ \sin m\omega_r \end{pmatrix} \Phi(\rho_r) d\rho_r d\zeta_r \quad (28b)$$

Similarly, for the stator the vector functions are

$$2\pi \begin{pmatrix} \vec{H}_0 \\ \equiv \\ \vec{H}_m \end{pmatrix} = \int_{R_{sr}h_s}^{R_{sr}} \int_{z_{s1}}^{z_{s2}} \vec{\mathcal{F}}_{1s}(\vec{r}_1, \vec{\rho}_s) \begin{pmatrix} \cot \frac{\omega_s}{2} \\ \equiv \\ \sin m\omega_s \end{pmatrix} \Psi_*(\rho_s) d\rho_s d\zeta_s \quad (28c)$$

$$2\pi \begin{pmatrix} \vec{J}_0 \\ \equiv \\ \vec{J}_m \end{pmatrix} = \int_{R_{sr}h_s}^{R_{sr}} \int_{z_{s1}}^{z_{s2}} \vec{\mathcal{F}}_{2s}(\vec{r}_1, \vec{\rho}_s) \begin{pmatrix} \cot \frac{\omega_s}{2} \\ \equiv \\ \sin m\omega_s \end{pmatrix} \Psi_*(\rho_s) d\rho_s d\zeta_s \quad (28d)$$

The vector functions $\vec{\mathcal{F}}_{1r}$, $\vec{\mathcal{F}}_{1s}$, $\vec{\mathcal{F}}_{2r}$, and $\vec{\mathcal{F}}_{2s}$ are defined by

$$\left. \begin{aligned} \vec{\mathcal{F}}_{1r} &= \frac{-\vec{i}(z - \zeta_r) \sin \psi_r + \vec{j}(z - \zeta_r) \cos \psi_r - \vec{k}r \sin(\theta - \psi_r)}{R_r^3(\vec{r}_1, \vec{\rho}_r)} \\ \vec{\mathcal{F}}_{2r} &= \frac{\vec{i}(r \cos \theta - \rho_r \cos \psi_r) + \vec{j}(r \sin \theta - \rho_r \sin \psi_r) + \vec{k}(z - \zeta_r)}{R_r^3(\vec{r}_1, \vec{\rho}_r)} \\ \vec{\mathcal{F}}_{1s} &= \frac{-\vec{i}(z - \zeta_s) \sin \psi_s + \vec{j}(z - \zeta_s) \cos \psi_s - \vec{k}r \sin(\theta - \psi_s)}{R_s^3(\vec{r}_1, \vec{\rho}_s)} \\ \vec{\mathcal{F}}_{2s} &= \frac{\vec{i}(r \cos \theta - \rho_s \cos \psi_s) + \vec{j}(r \sin \theta - \rho_s \sin \psi_s) + \vec{k}(z - \zeta_s)}{R_s^3(\vec{r}_1, \vec{\rho}_s)} \end{aligned} \right\} \quad (29)$$

with

$$\left. \begin{aligned} R_r(\vec{r}_1, \vec{\rho}_r) &= \left[(r_1 - \rho_r)^2 + (z_1 - \zeta_r)^2 - 4r\rho_r \cos^2 \frac{1}{2}(\theta - \psi_r) \right]^{1/2} \\ R_s(\vec{r}_1, \vec{\rho}_s) &= \left[(r_1 - \rho_s)^2 + (z_1 - \zeta_s)^2 - 4r\rho_s \cos^2 \frac{1}{2}(\theta - \psi_s) \right]^{1/2} \end{aligned} \right\} \quad (30)$$

Besides considering the induced velocity of the bound vortices in the rotor and stator, it is also necessary to include the induced velocity of the trailing vortices shed by the rotor and stator. These vortices move downstream along helical paths. The trailing vortices shed by the stator blades are opposite in their sense of rotation to those shed by the rotor blades. Furthermore, when the rotor and stator have nearly equal reactions, the trailing vortices of both the rotor and stator may be assumed to be nearly equal in strength at all radii. Thus the net vorticity downstream of the stator is assumed to be nearly zero. Furthermore, because of the close spacing between the rotor and the stator, the effect of the vortices shed by the rotor in the rotor-stator gap will also be neglected. Consequently the

induced velocity \vec{u} of equation (26) is the complete induced velocity of the stage.

MATCHING OF ROTOR AND STATOR FLOW FIELDS

The perturbation velocities $\vec{u}(\vec{r}, t)$ and the resulting perturbation pressures given in the preceding section at a point \vec{r} in the flow field are based on the hypothesis that the individual contributions of the rotor and stator are additive and are not vitiated by the interaction effects between them. The singularity distributions on the blade surfaces assumed in equations (2) imply no rotor-stator interference and satisfy, individually, the Kutta condition at the trailing edge of both the rotor and stator. However, the flow tangency condition is disturbed when the rotor and stator are juxtaposed closely to form a compressor stage.

It is necessary to satisfy the flow tangency condition for the combination simultaneously. This can be done by introducing an interference velocity

\vec{u}_{rs} and the corresponding interference pressure p_{rs} so that the resultant induced velocity vector \vec{v} and the resultant perturbation pressure p are written as

$$\vec{v} = \vec{u} + \vec{u}_{rs}; \quad \hat{p} = p + p_{rs} \quad (31)$$

Under the hypothesis of small perturbations the interference velocity \vec{u}_{rs} is assumed to be a constant fraction ϵ of the induced velocity \vec{u} of the rotor and stator

$$\vec{v} = (1 + \epsilon)\vec{u} \quad (32)$$

From the lifting-line model it is known that the strength of the bound vortex is a maximum at the blade root for both the rotor and the stator. A vortex filament of this maximum strength extends downstream to infinity from the root of each blade. If Γ_{rh} and Γ_{sh} be the strength of the blade root vorticity per blade of the rotor and stator, respectively, the condition of zero net vorticity behind the stator blade becomes

$$Z_r \Gamma_{rh} + Z_s \Gamma_{sh} = 0 \quad (33)$$

This equation provides the necessary condition for determining the set of expansion coefficients in the Glauert series and the interaction factor ϵ . The vortex strengths Γ_{rh} and Γ_{sh} are obtained by a chordwise integration of the surface density of vorticity in equation (11) so that we have

$$\Gamma_{rh} = \sum_{m=0}^{\infty} \hat{A}_m E_{rm}(h_r); \quad \Gamma_{sh} = \sum_{m=0}^{\infty} \hat{C}_m E_{sm}(h_s) \quad (34)$$

where $E_{rm}(h_r)$ and $E_{sm}(h_s)$ are defined by

$$\left. \begin{aligned} E_{r0}(h_r) &= S_{rh} \int_0^{\pi} \cot \frac{\omega_r}{2} d\zeta_r; & E_{rm}(h_r) &= S_{rh} \int_0^{\pi} \sin m\omega_r d\zeta_r \\ E_{s0}(h_s) &= S_{sh} \int_0^{\pi} \cot \frac{\omega_s}{2} d\zeta_s; & E_{sm}(h_s) &= S_{sh} \int_0^{\pi} \sin m\omega_s d\zeta_s \end{aligned} \right\} \quad (35)$$

with S_{rh} and S_{sh} obtained from equation (9) by setting r_1 equal to h_r and $R_{sr}h_s$ for the rotor and stator so that

$$S_{rh}(h_r) = \Phi_*(h_r); \quad S_{sh}(R_{sr}h_s) = \Psi_*(R_{sr}h_s) \quad (36)$$

Equation (35) can be integrated and rewritten as

$$\left. \begin{aligned} E_{r0}(h_r) &= -2\pi C_R S_{rh}(h_r) \cos \alpha_r; & E_{s0}(h_s) &= -2\pi C_S S_{sh}(R_{sr}h_s) \cos \alpha_s \\ E_{r1}(h_r) &= -\pi C_R S_{rh}(h_r) \cos \alpha_r; & E_{s1}(h_s) &= -\pi C_S S_{sh}(R_{sr}h_s) \cos \alpha_s \\ E_{rm}(h_r) &= 0; & E_{sm}(h_s) &= 0 \quad m = 2, 3, \dots, \infty \end{aligned} \right\} \quad (37)$$

BOUNDARY CONDITIONS

For compressors and fans with small tip clearances, the combined perturbation velocity field \vec{v} of equation (32) together with the gross velocities of the free stream must satisfy the condition of no radial flow at both the hub and tip of the rotor and stator. Furthermore, both the rotor- and stator-blade surfaces must be stream surfaces. The latter condition is convenient to apply while dealing with the resultant velocity field of the flow singularities.

The gross free-stream velocities $\vec{V}_R(0, V_R, W_R)$ and $\vec{V}_S(0, V_S, W_S)$ for the rotor and stator assumed in the Introduction together with the resultant perturbation velocity \vec{v} of equation (32) give the resultant total velocity \vec{U}_R, \vec{U}_S

$$\vec{U}_R = \vec{V}_R + \vec{v}; \quad \vec{U}_S = \vec{V}_S + \vec{v} \quad (38)$$

where $\vec{U}_R, \vec{U}_S, \vec{V}_R$, and \vec{V}_S are velocities renormalized in such a way that

$$\left. \begin{aligned} \vec{U}_R &= \vec{U}_R/W_a; & \vec{U}_S &= \vec{U}_S/W_a \\ \vec{V}_R &= \vec{V}_R/W_a; & \vec{V}_S &= \vec{V}_S/W_a \end{aligned} \right\} \quad (39)$$

whose Cartesian components for any azimuth angle ψ_r, ψ_s on the rotor and stator are given by

$$\left. \begin{aligned} \vec{V}_R &= \left[\frac{r_1}{R_+} \sin \psi_r; \quad -\frac{r_1}{R_+} \cos \psi_r; \quad 1 \right] \\ \vec{V}_S &= \left[\left(\frac{r_1}{R_+} + \tan \alpha_2 \right) \sin \psi_s; \quad \left(\frac{r_1}{R_+} + \tan \alpha_2 \right) \cos \psi_s; \quad 1 \right] \\ \vec{U}_R &= \left[\frac{r_1}{R_+} \sin \psi_r + \hat{v}_x; \quad -\frac{r_1}{R_+} \cos \psi_r + \hat{v}_y; \quad 1 + \hat{v}_z \right] \\ \vec{U}_S &= \left[\left(\frac{r_1}{R_+} + \tan \alpha_2 \right) \sin \psi_s + \hat{v}_x; \quad \left(\frac{r_1}{R_+} + \tan \alpha_2 \right) \cos \psi_s + \hat{v}_y; \quad 1 + \hat{v}_z \right] \end{aligned} \right\} \quad (40)$$

where $R_+ = (W_a/\Omega r_{tr})$ is a characteristic dimensionless radius. R_+ may also be regarded as the advance ratio of the blade based on the tip radius of the rotor. Assuming that the incoming flow is uniform in front of the rotor, the flow characteristics at any point of the blade surface are only peculiar to its radial location on an arbitrary blade. The same condition applies, likewise, to the stator blade. Therefore the angles ψ_r and ψ_s given by equations (14) and (17) can be replaced by φ_r and φ_s , respectively, and the midchord line of the blade may be considered to be parallel to the X-axis.

The resultant velocities \vec{u}_R and \vec{u}_S can be resolved along and perpendicular to the blade chord in terms of the local coordinates ($Y' - Z'$) mentioned in the section Representation of Lifting Surface. To be consistent with the postulates of thin-aerofoil theory, the boundary condition is applied at the blade chord. The resultant velocities are given by

$$\left. \begin{aligned}
\hat{U}_{Ry'} &= \left(\frac{r_1}{R_+} + \hat{v}_x \sin \varphi_r + \hat{v}_y \cos \varphi_r \right) \sin \alpha_r + (1 + \hat{v}_z) \cos \alpha_r \\
\hat{U}_{Rz'} &= \left(\frac{r_1}{R_+} + \hat{v}_x \sin \varphi_r + \hat{v}_y \cos \varphi_r \right) \cos \alpha_r - (1 + \hat{v}_z) \sin \alpha_r \\
\hat{U}_{Sy'} &= - \left(\frac{r_1}{R_+} + \tan \alpha_2 + \hat{v}_x \sin \varphi_s + \hat{v}_y \cos \varphi_s \right) \sin \alpha_s + (1 + \hat{v}_z) \cos \alpha_s \\
\hat{U}_{Sz'} &= \left(\frac{r_1}{R_+} + \tan \alpha_2 + \hat{v}_x \sin \varphi_s + \hat{v}_y \cos \varphi_s \right) \cos \alpha_s + (1 + \hat{v}_z) \sin \alpha_s
\end{aligned} \right\} \quad (41)$$

wherein we have neglected terms of second order and higher in $\hat{v}_x, \hat{v}_y, \hat{v}_z$. The resultant perturbation velocity components \hat{v}_R and \hat{v}_S at the rotor and stator in the local coordinate system are related to those in the Cartesian system by the matrix transformation

$$\begin{bmatrix} \hat{v}_{Rr} \\ \hat{v}_{Ry'} \\ \hat{v}_{Rz'} \\ \hat{v}_{Sr} \\ \hat{v}_{Sy'} \\ \hat{v}_{Sz'} \end{bmatrix} = \begin{bmatrix} \cos \varphi_r & \sin \varphi_r & 0 \\ \sin \varphi_r \sin \alpha_r & \cos \varphi_r \sin \alpha_r & \cos \alpha_r \\ \sin \varphi_r \cos \alpha_r & \cos \varphi_r \cos \alpha_r & -\sin \alpha_r \\ \cos \varphi_s & \sin \varphi_s & 0 \\ -\sin \varphi_s \sin \alpha_s & -\cos \varphi_s \sin \alpha_s & \cos \alpha_s \\ \sin \varphi_s \cos \alpha_s & \cos \varphi_s \cos \alpha_s & \sin \alpha_s \end{bmatrix} \begin{bmatrix} \hat{v}_x \\ \hat{v}_y \\ \hat{v}_z \end{bmatrix} \quad (42)$$

While calculating the perturbation velocities \vec{v}_R and \vec{v}_S in the blade coordinates at the rotor and stator given by the column matrix on the left of equation (42), it is to be noted that the Cartesian velocity components ($\hat{v}_x, \hat{v}_y, \hat{v}_z$) are evaluated at the corresponding points on the rotor and stator, respectively. The kinematical flow conditions of flow tangency on the blade surface at any radius r_1 can now be expressed as

$$\begin{aligned}
\left(\frac{dz'_c}{dy'} \right)_r &= \frac{\hat{U}_{Rz'}}{\hat{U}_{Ry'}} \bigg|_{z'_r=0} ; & \left(\frac{dz'_T}{dy'} \right)_r &= \frac{1}{2} \frac{\hat{Q}_r}{\hat{U}_{Ry'}} \bigg|_{z'_r=0} \\
\left(\frac{dz'_c}{dy'} \right)_s &= \frac{\hat{U}_{Sz'}}{\hat{U}_{Sy'}} \bigg|_{z'_s=0} ; & \left(\frac{dz'_T}{dy'} \right)_s &= \frac{1}{2} \frac{\hat{Q}_s}{\hat{U}_{Sy'}} \bigg|_{z'_s=0}
\end{aligned} \quad (43)$$

To be consistent with the postulates of thin-aerofoil theory, in equations (43) the boundary conditions are satisfied at the local chord of the blade by setting $z'_r = 0$ or $z'_s = 0$ as appropriate to the blade in question.

From these considerations and equation (12) at any given radius a relation between the azimuth angles (φ_r, z_r, r_1) and (φ_s, z_s, r_1) is obtained as

$$\tan \varphi_r = \frac{(z_{r0} - z_r) \tan \alpha_r}{r_1}; \quad \tan \varphi_s = \frac{(z_s - z_{s0}) \tan \alpha_s}{r_1} \quad (44)$$

These can be substituted for z_r and z_s in the expressions of equations (43).

The slopes of the mean camber line and the thickness distribution for the rotor and stator blades as given by the derivatives on the left of equations (43) are known for given blade profiles. These derivatives are denoted as

$$\left. \begin{aligned} \tau_{rc} &= \left(\frac{dz'_c}{dy'_i} \right)_r; & \tau_{rT} &= 2 \left(\frac{dz'_T}{dy'_i} \right)_r \\ r_{sc} &= \left(\frac{dz'_c}{dy'_i} \right)_s; & \tau_{sT} &= 2 \left(\frac{dz'_T}{dy'_i} \right)_s \end{aligned} \right\} \quad (45)$$

Combining equations (42) and (43) with equation (3) gives, after some simplification,

$$\begin{aligned} \frac{r_1}{R} + \hat{v}_x \sin \varphi_r + \hat{v}_y \cos \varphi_r - (1 + \hat{v}_z) \left(\frac{\sin \alpha_r + \tau_{rc} \cos \alpha_r}{\cos \alpha_r - \tau_{rc} \sin \alpha_r} \right) &= 0 \\ \frac{r_1}{R} + \tan \alpha_2 + \hat{v}_x \sin \varphi_s + \hat{v}_y \cos \varphi_s + (1 + \hat{v}_z) \left(\frac{\sin \alpha_s - \tau_{sc} \cos \alpha_s}{\cos \alpha_s + \tau_{sc} \sin \alpha_s} \right) &= 0 \\ \left(\frac{r_1}{R} + \hat{v}_x \sin \varphi_r + \hat{v}_y \cos \varphi_r \right) \tan \varphi_r + (1 + \hat{v}_z) &= \sum_{m=0}^{\infty} \hat{B}_m T_{rm}(r_1) \\ \left(\frac{r_1}{R} + \tan \alpha_2 + \hat{v}_x \sin \varphi_s + \hat{v}_y \cos \varphi_s \right) \tan \varphi_s + (1 + \hat{v}_z) &= - \sum_{m=0}^{\infty} \hat{D}_m T_{sm}(r_1) \end{aligned} \quad (46)$$

where

$$\left. \begin{aligned} T_{r0}(r_1) &= \frac{\Phi(r_1)}{\tau_{rT}} \cot \frac{\omega_r}{2}; & T_{s0}(r_1) &= \frac{\Psi(r_1)}{\tau_{sT}} \cot \frac{\omega_s}{2} \\ T_{rm}(r_1) &= \frac{\Phi(r_1)}{\tau_{rT}} \sin m\omega_r; & T_{sm}(r_1) &= \frac{\Psi(r_1)}{\tau_{sT}} \sin m\omega_s \\ T_{r1} &= -2 \frac{\Phi(r_1)}{\tau_{rT}} \sin \omega_r; & T_{s1} &= -2 \frac{\Psi(r_1)}{\tau_{sT}} \sin \omega_s \end{aligned} \right\} \quad (47)$$

DETERMINATION OF CONSTANTS

The nature of the distribution of the flow singularities on the blade surface depends on the coefficients A_m , B_m , C_m , and D_m ($m = 0, 1, 2, \dots, \infty$) in equations (2). To determine these coefficients, the surface boundary conditions in equations (46) have been introduced. Substituting for the resultant induced velocities \hat{v}_x , \hat{v}_y , and \hat{v}_z from equations (32) and (26) and combining the different quantities give for each point on the blade the following set of simultaneous algebraic equations:

$$\left. \begin{aligned} \sum_{m=0}^{\infty} \hat{A}_m \mathcal{F}_{1m} + \hat{B}_m \mathcal{G}_{1m} + \hat{C}_m \mathcal{H}_{1m} + \hat{D}_m \mathcal{J}_{1m} + \frac{r_1/R_+ - g_r}{1 + \epsilon} &= 0 \\ \sum_{m=0}^{\infty} \hat{A}_m \mathcal{F}_{2m} + \hat{B}_m \mathcal{G}_{2m} + \hat{C}_m \mathcal{H}_{2m} + \hat{D}_m \mathcal{J}_{2m} + \frac{r_1/R_+ + \tan \alpha_2 - g_s}{1 + \epsilon} &= 0 \\ \sum_{m=0}^{\infty} \hat{A}_m \mathcal{F}_{3m} + \hat{B}_m \mathcal{G}_{3m} + \hat{C}_m \mathcal{H}_{3m} + \hat{D}_m \mathcal{J}_{3m} + \frac{1 + r_1/R_+ \tan \alpha_r}{1 + \epsilon} &= \sum_{m=0}^{\infty} \frac{B_m T_{rm}}{1 + \epsilon} \\ \sum_{m=0}^{\infty} \hat{A}_m \mathcal{F}_{4m} + \hat{B}_m \mathcal{G}_{4m} + \hat{C}_m \mathcal{H}_{4m} + \hat{D}_m \mathcal{J}_{4m} + \frac{1 + r_1/R_+ + \tan \alpha_2}{1 + \epsilon} &= - \sum_{m=0}^{\infty} \frac{\hat{D}_m T_{sm}}{1 + \epsilon} \end{aligned} \right\} \quad (48)$$

where g_r and g_s are defined by the relations

$$\left. \begin{aligned} g_r(\omega_r) &= \frac{\sin \alpha_r + \tau_{rc} \cos \alpha_r}{\cos \alpha_r - \tau_{rc} \sin \alpha_r} \\ g_s(\omega_s) &= \frac{\sin \alpha_s + \tau_{sc} \cos \alpha_s}{\cos \alpha_s - \tau_{sc} \sin \alpha_s} \end{aligned} \right\} \quad (49)$$

and the set of functions \mathcal{F} , \mathcal{G} , \mathcal{H} , and \mathcal{J} by the matrix relations

$$\left. \begin{aligned} \mathcal{F}_m &= SR * F_m; & \mathcal{G}_m &= SR * G_m \\ \mathcal{H}_m &= Sr * H_m; & \mathcal{J}_m &= SR * J_m \end{aligned} \right\} \quad (50)$$

The matrix SR and the column vectors F_m , G_m , H_m , J_m , \mathcal{F}_m , \mathcal{G}_m , \mathcal{H}_m , and \mathcal{J}_m are given by

$$SR = \begin{bmatrix} \sin \varphi_r & \cos \varphi_r & -g_r \\ \sin \varphi_s & \cos \varphi_s & +g_s \\ \sin \varphi_r \tan \alpha_r & \cos \varphi_r \tan \alpha_r & 1 \\ \sin \varphi_s \tan \alpha_s & \cos \varphi_s \tan \alpha_s & -1 \end{bmatrix} \quad (51)$$

$$\vec{F}_m = \begin{bmatrix} F_{mx} \\ F_{my} \\ F_{mz} \end{bmatrix}; \quad \vec{G}_m = \begin{bmatrix} G_{mx} \\ G_{my} \\ G_{mz} \end{bmatrix}; \quad \vec{H}_m = \begin{bmatrix} H_{mx} \\ H_{my} \\ H_{mz} \end{bmatrix}; \quad \vec{J}_m = \begin{bmatrix} J_{mx} \\ J_{my} \\ J_{mz} \end{bmatrix} \quad (52)$$

$$\mathcal{F}_m = \begin{bmatrix} \mathcal{F}_{1m} \\ \mathcal{F}_{2m} \\ \mathcal{F}_{3m} \\ \mathcal{F}_{4m} \end{bmatrix}; \quad \mathcal{G}_m = \begin{bmatrix} \mathcal{G}_{1m} \\ \mathcal{G}_{2m} \\ \mathcal{G}_{3m} \\ \mathcal{G}_{4m} \end{bmatrix}; \quad \mathcal{H}_m = \begin{bmatrix} \mathcal{H}_{1m} \\ \mathcal{H}_{2m} \\ \mathcal{H}_{3m} \\ \mathcal{H}_{4m} \end{bmatrix}; \quad \mathcal{J}_m = \begin{bmatrix} \mathcal{J}_{1m} \\ \mathcal{J}_{2m} \\ \mathcal{J}_{3m} \\ \mathcal{J}_{4m} \end{bmatrix} \quad (53)$$

for $m = 0, 1, 2, \dots, \infty$. The coefficients \hat{A}_m , \hat{B}_m , \hat{C}_m , and \hat{D}_m can be determined from the set of equations (48). However, since the interaction parameter ϵ is unknown, an additional equation must be provided. This is done by adjoining equation (33) to equation (48), which provides the matching of the rotor and the stator. By combining equations (33) and (34), the additional equation becomes

$$\sum_{m=0}^{\infty} [\hat{A}_m Z_r E_{rm} + \hat{C}_m Z_s E_{sm}] = 0 \quad (54)$$

with $E_{rm}(h_r)$ and $E_{sm}(h_s)$ defined by equations (35). Thus equations (48) and (54) are the set of simultaneous equations to be solved in order to determine the infinite set of constants \hat{A}_m , \hat{B}_m , \hat{C}_m , and \hat{D}_m and the interference parameter ϵ .

Discretization of Problem

It is seen from equations (48) and (54) that the infinite set of coefficients \hat{A}_m , \hat{B}_m , \hat{C}_m , and \hat{D}_m is, indeed, required to describe the flow over the rotor- and stator-blade surfaces for each value of r_1 and results in infinite matrices. The dimensions of the problem can be reduced by selecting a finite number of terms $m = (M^* - 1)$ in the Glauert series of equations (2) for both the rotor and the stator so that $4M^* + 1$ unknown constants must be determined. As for the blade surface, R^* stations over the blade length and N^* points along the blade chord are considered at which the camber and thickness profiles and their slopes are specified for both the rotor and stator. Thus the number of terms in each of equations (2) equals $M^* = R^*N^*$ and the matrix of the coefficients \hat{A} , \hat{B} , \hat{C} , and \hat{D}_m is of order $4M^*$.

The chordwise location of the points can be obtained by using the 3/4-chord theorem for each chord segment. Thus, since the midpoint of the chord has been chosen for each chord reference for $N^* = 4$, these points will be located at $(-5/16, -1/16, 3/16, 7/16)$ of the dimensionless rotor and stator chords C_r and C_s , respectively. For $R^* = 3$, the radial location of the points would be $r_1 = [h_r, (1 + h_r)/2, 1]$ on the rotor and $r_1 = [R_{sr}h_s, R_{sr}(1 + h_s)/2, R_{sr}]$ on the stator, corresponding to the hub, mean, and tip, respectively, of each blade.

The set of equations (48) and (54) can be written as a single matrix equation

$$EF * AA = (EE * AA)\epsilon_1 \quad (55)$$

where EF is a $(4M^* + 1)$ -order square matrix of the integrals \mathcal{F} , \mathcal{G} , \mathcal{H} , and \mathcal{J} and the blade geometry parameters; AA is the $(4M^* + 1)$ -order column vector of the constants \hat{A}_m , \hat{B}_m , \hat{C}_m , \hat{D}_m , and ϵ_1 , where

$$\epsilon_1 = \frac{1}{1 + \epsilon} \quad (56)$$

and the matrices EF , AA , and EE are defined by

$$EF = \left[\begin{array}{cccc|c} \mathcal{F} & \mathcal{G} & \mathcal{H} & \mathcal{J} & EM \\ \hline Z_m E_{rm} & 0 & Z_m E_{sm} & 0 & 0 \end{array} \right] \quad (57)$$

$$AA = [\mathcal{A} \ \mathcal{B} \ \mathcal{C} \ \mathcal{D} \ \epsilon_1]^T \quad (58)$$

$$EE = \left[\begin{array}{cccc|c} 0 & 0 & 0 & 0 & 0 \\ 0 & 0 & T_{rm} & 0 & 0 \\ 0 & 0 & 0 & 0 & 0 \\ 0 & 0 & 0 & T_{sm} & 0 \\ \hline 0 & 0 & 0 & 0 & 0 \end{array} \right] \quad (59)$$

The submatrices \mathcal{F} , \mathcal{G} , \mathcal{H} , and \mathcal{J} are each of order $(4M^* \times M^*)$; EM is a $(4M^* \times 1)$ -order column matrix with each block of elements EM_1 , EM_2 , EM_3 , and EM_4 given by

$$EM_1 = \left(\frac{r_1}{R_+} - g_r \right); \quad EM_2 = \left(\frac{r_1}{R_+} + \tan \alpha_{2r} + g_s \right) \quad (60)$$

$$EM_3 = \left(1 + \frac{r_1}{R_+} \tan \alpha_r \right); \quad EM_4 = 1 + \left(\frac{r_1}{R_+} + \tan \alpha_{2r} \tan \right) \alpha_s$$

and

$$\begin{aligned} \mathcal{A} &= [\hat{A}_0 \ \dots \ \hat{A}_{M^*-1}]; & \mathcal{B} &= [\hat{B}_0 \ \dots \ \hat{B}_{M^*-1}] \\ \mathcal{C} &= [\hat{C}_0 \ \dots \ \hat{C}_{M^*-1}]; & \mathcal{D} &= [\hat{D}_0 \ \dots \ \hat{D}_{M^*-1}] \end{aligned} \quad (61)$$

are $(1 \times M^*)$ -order row vectors; and $Z_r E_{rm}$ and $Z_s E_{sm}$ are $(1 \times M^*)$ row vectors. The matrix EE has only two nonnull submatrices, $T_{rm}/\tau_r T$ and $-T_{sm}/\tau_s T$, each of order $(M^* \times M^*)$.

It is observed from equations (48) that the unknown interaction parameter ϵ_1 multiplies the unknown coefficient matrix AA of which ϵ_1 is also an element. In this sense, the matrix equation (55) is nonlinear. The equation

can be solved by an iteration process that assumes $\epsilon < 1$ and expands in powers of ϵ so that

$$\epsilon_1 = (1 + \epsilon)^{-1} = 1 - \epsilon + \epsilon^2 - \epsilon^3 + \dots \quad (62)$$

Equation (55) can also be written

$$EF * AA = (EE * AA)(1 - \epsilon + \epsilon^2 - \epsilon^3 + \dots) \quad (63)$$

By setting $\epsilon = 0$, the zeroth-order solution $AA^{(0)}$ is obtained from the eigenvectors AA of the matrix equation

$$EF * AA = EE * AA \quad (64)$$

from which $\epsilon_1^{(0)}$ to zeroth order is obtained. This can be used to obtain the first-order $\epsilon_1^{(1)}$, and a first-order vector $AA^{(1)}$ can be obtained from the equation

$$EF * AA = (1 - \epsilon^{(1)})(EE * AA) \quad (65)$$

This matrix iteration process can be continued until the changes in the succeeding values of ϵ_1 or ϵ and the eigenvectors are within acceptable limits. The eigenvectors provide the constants used in the distribution of flow singularities over the blade surface.

NET PRESSURE DISTRIBUTION ON LIFTING SURFACE

From the results obtained in the preceding section for \vec{u} and \vec{v} , including the effects of rotor-stator interaction, it is possible to obtain the local static pressure on the blade. Thus, if p_{0r} and p_{0s} be the total pressures ahead of the rotor and stator with the corresponding air density ρ , the Bernoulli equation gives

$$p_{0r} - p_r = \frac{1}{2}(V_r^2 - W_a^2); \quad p_{0s} - p_s = \frac{1}{2}(V_s^2 - W_s^2) \quad (66)$$

where V_r and V_s are the corresponding local velocities. Using equations (40) for the resultant velocities U_r and U_s at the rotor and stator and neglecting the quadratic terms \hat{v}_x^2 , \hat{v}_y^2 , and \hat{v}_z^2 give

$$\frac{p_\infty - p}{\frac{1}{2}\rho W_a^2} = 2\left(\frac{r_1}{R_+} \hat{v}_\theta + \hat{v}_z\right)_r; \quad \frac{p_\infty - p}{\frac{1}{2}\rho W_a^2} = 2\left[\left(\frac{r_1}{R_+} - \tan \alpha_2\right) \hat{v}_r + \hat{v}_z\right] \quad (67)$$

The net pressure distribution on the blades, defined as the difference between the upper and lower surfaces of the blades, can be obtained from equations (67) to the first order in the induced velocities \hat{v}_x , \hat{v}_y , and \hat{v}_z as

$$\begin{aligned} \frac{\Delta p_r}{q} &= \left(\frac{r_1}{R_+} \sin \alpha_r + \cos \alpha_r \right) (\hat{v}'_{yL} - \hat{v}'_{yU}) - \left(\frac{r_1}{R_+} \cos \alpha_r - \sin \alpha_r \right) (\hat{v}'_{zL} - \hat{v}'_{zU}) \\ \frac{\Delta p_s}{q} &= \left[\left(\frac{r_1}{R_+} - \tan \alpha_2 \right) \sin \alpha_s + \cos \alpha_s \right] (\hat{v}'_{yL} - \hat{v}'_{yU}) \\ &\quad - \left[\left(\frac{r_1}{R_+} - \tan \alpha_2 \right) \cos \alpha_s - \sin \alpha_s \right] (\hat{v}'_{yL} - \hat{v}'_{zU}) \end{aligned} \quad (68)$$

where \hat{v}'_U and \hat{v}'_L are, respectively, the total induced-velocity vectors on the upper and lower surfaces of the blades evaluated at the chordline of the rotor and stator blades as required.

The local lift coefficients C_{lr} and C_{ls} of the rotor and stator blades are defined by

$$C_{lr} = \frac{L_r}{q(1 + r_1^2/R_+^2)2C_r}; \quad C_{ls} = \frac{L_s}{q(1 + r_1^2/R_+^2)2C_s} \quad (69)$$

where L_r and L_s are the local lift per unit span of the rotor and stator blades and can be expressed in terms of Δp_r and Δp_s as

$$L_r = \int_{z_{r1}}^{z_{r2}} \Delta p_r dz_1; \quad L_s = \int_{z_{s1}}^{z_{s2}} \Delta p_s dz_1 \quad (70)$$

Since the flow field of the stage is complex, it would be convenient to define the upwash as the axial component of the induced velocity. Because of the nature of the chordwise distribution of circulation given in equations (9), the magnitude of the upwash velocity on the rotor depends on the chordwise position of the rotor point considered. Let us consider the upwash velocity at the midpoint of the rotor-blade chord at the median plane. From equation (26) the upwash velocity is obtained as

$$\hat{u}_z = \sum_{m=0}^{\infty} (\hat{A}_m F_{mz} + \hat{B}_m G_{mz} + \hat{C}_m H_{mz} + \hat{D}_m J_{mz}) \Big|_{z=z_R} \quad (71)$$

which is a function of the radial position r_1 along the blade. Since the blade loading increases toward the blade tip, the blade tips will probably be closer to stall with the stator than without.

DISCUSSION

This report is primarily of a theoretical nature, outlining the methodology for including the stator of a turbomachine to make a combined study of

the rotor and stator as a subsystem. The lifting-surface theory outlined here provides a proper framework for the analysis. The theory can be applied to several interesting cases. Thus the case of an isolated rotor can be discussed by putting $Z_S = 0$. The solution for a single actuator disk can be obtained by letting $Z_r \rightarrow \infty$ and $Z_S = 0$ while allowing the lift force per rotor blade to tend toward zero. The flow field of a pair of infinite, two-dimensional cascades in parallel is obtained for $h_r \rightarrow 1$; $h_S \rightarrow 1$.

It is seen from the method used to represent the lifting-surface of the rotor and stator that each additional row of blades introduces two more sets of coefficients in the corresponding Glauert series expansion. The overall aerodynamic interaction effect of additional rows on the first row can still be represented by ϵ . Keeping the same number of R_* stations over the blade length and N_* points along the blade chord for specifying the blade surface geometry results in the size of the matrix involved in determining the Glauert series coefficients being $2 \times \text{number of rows} \times R_* N_* + 1$.

The Bessel functions employed above in the distribution of the flow singularities extend to very high orders, for which asymptotic representations are important for numerical evaluation. This aspect will be discussed along with the results for a stage of given geometry and flow condition and compared with measurements in a separate report.

CONCLUDING REMARKS

The application of the lifting-surface theory for a complete stage of a turbomachine of arbitrary camber, thickness, and other cascade geometry parameters has been demonstrated for arbitrary flow conditions with subsonic axial flow. The separation of the rotor-stator interference effect has also been shown. Expressions have been given for the spanwise loading on the individual blades for uniform steady inlet flow.

REFERENCES

1. Traupel, W., "Neue Allgemeine Theorie der Mehrstufigen Axialen Turbomaschinen," verif. Engl. Translation: Traupel, Walter (Dr. C. W. Smith, transl.): New General Theory of Multistage Axial Flow Turbomachines. Navy Department. Lieman & Co., Zurich, 1942.
2. Marble, Frank E.: The Flow of a Perfect Fluid Through an Axial Turbomachine with Prescribed Blade Loading. J. Aeronaut. Sci., vol. 15, no. 8, Aug. 1948, pp. 473-485.
3. Marble, Frank E.; and Michelson, Irving: Analytical Investigation of Some Three-Dimensional Flow Problems in Turbomachines. NACA TN-2614, 1952.
4. Raily, J.W.: The Flow of an Incompressible Fluid Through an Axial Turbomachine with Any Number of Rows. Aero. Quart., vol. 3, Sept. 1951, pp. 133-144.
5. Horlock, J.H.: Some Actuator-Disc Theories for the Flow of Air Through an Axial Turbomachine. R&M 3030, 1958.

6. Horlock, J.H.; and Deverson, E.C.: An Experiment to Determine the Position of an Equivalent Actuator Disc Replacing a Blade Row of a Turbomachine. ARC CP-426, 1959.
7. Kemp, Nelson H.; and Sears, W.R.: Aerodynamic Interference Between Moving Blade Rows. J. Aeronaut. Sci., vol. 20, no. 9, Sept. 1953, pp. 585-597.
8. Kemp, Nelson H.; and Sears, W.R.: The Unsteady Forces Due to Viscous Wakes in Turbomachines. J. Aeronaut. Sci., vol. 22, no. 7, July 1955, pp. 478-483.
9. Prandtl, Ludwig; and Betz, Albert: Vier Abhandlungen zur Hydrodynamik und Aerodynamik. Flüssigkeit mit kleiner Reibung; Tragflugeltheorie, I. und II. Mitteilung; Schraubenpropeller mit geringstem Energieverlust. Selbstverlag des Kaiser Wilhelm - Instituts für Strömungsforschung (Göttingen), 1927.
10. Goldstein, S.: On the Vortex Theory of Screw Propellers. Proc. Roy Soc. London, Ser. A, vol. 123, Apr. 1929, pp. 440-465.
11. Busemann, Adolf: Theory of the Propeller in Compressible Flow. Proceedings of the Third Mid-Western Conference on Fluid Mechanics, Minneapolis, Minn., 1953, pp. 267-286.
12. Davidson, Robert E.: Linearized Potential Theory of Propeller Induction in a Compressible Flow. NACA TN-2983, 1953.
13. Rott, N.: On Wave Radiation in Compressible Flow Through an Axial Compressor. Phys. Rev., vol. 84, no. 3, Nov. 1, 1951, p. 613.
14. McCune, James Elliot: The Three-Dimensional Flow Field of an Axial Compressor Blade Row - Subsonic, Transonic, and Supersonic. Ph.D. Thesis, Cornell Univ., 1958.
15. McCune, James E.: A Three-Dimensional Theory of Axial Compressor Blade Rows - Application in Subsonic and Supersonic Flows. J. Aerosp. Sci., vol. 25, no. 9, Sept. 1958, pp. 544-560.
16. Okurounmu, Olufemi; and McCune, James E.: Three-Dimensional Vortex Theory of Axial Compressor Blade Rows at Subsonic and Transonic Speeds. AIAA J. vol. 8, no. 7, July 1970, pp. 1275-1283.
17. Namba, M.: Lifting Surface Theory for a Rotating Subsonic or Transonic Blades Row. R&M 3740, British ARC, 1974.
18. Wu, Ching-Hua: A General Theory of Three-Dimensional Flow in Subsonic and Supersonic Turbomachines of Axial-, Radial-, and Mixed-Flow Types. NACA TN-2604, 1952.
19. Schlichting, H.: Some Problems of Cascade Flow. Proceedings of the Conference on High Speed Aeronautics. Polytech. Inst., Brooklyn, New York, 1955, pp. 175-187.

20. Birnbaum, W.: Die Tragende Wirbel Fläche Als Hilfsmittel zur Behandlung des Ebenen Problems der Tragflügeltheorie. Z. Angew. Math. Mech., vol. 3, 1923, pp. 290-297.
21. Glauert, H.: The Elements of Aerofoil and Airscrew Theory. Second ed., Cambridge, University Press, 1947.

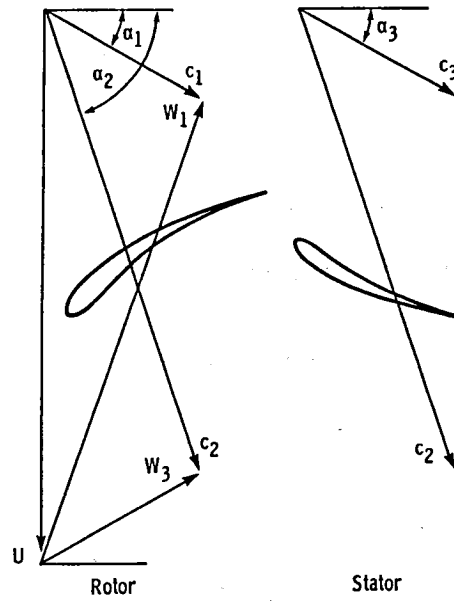


Figure 1. - Velocity diagram of stage.

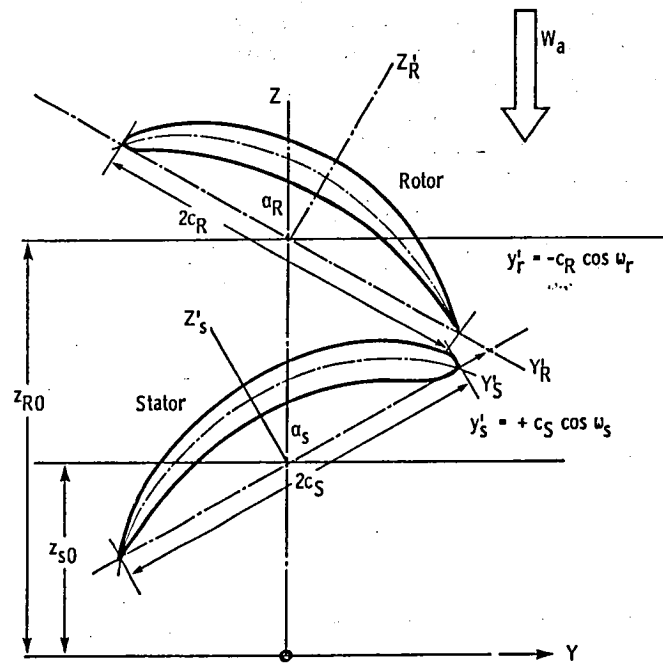


Figure 2. - Local coordinate system for blades of stage.

1. Report No. NASA TM-83767		2. Government Accession No.		3. Recipient's Catalog No.	
4. Title and Subtitle Incompressible Lifting-Surface Aerodynamics for a Rotor-Stator Combination				5. Report Date October 1984	
				6. Performing Organization Code 505-40-5A	
7. Author(s) Sridhar M. Ramachandra				8. Performing Organization Report No. E-2258	
				10. Work Unit No.	
9. Performing Organization Name and Address National Aeronautics and Space Administration Lewis Research Center Cleveland, Ohio 44135				11. Contract or Grant No.	
				13. Type of Report and Period Covered Technical Memorandum	
12. Sponsoring Agency Name and Address National Aeronautics and Space Administration Washington, D.C. 20546				14. Sponsoring Agency Code	
15. Supplementary Notes Sridhar M. Ramachandra, NRC-NASA Resident Research Associate.					
16. Abstract Current literature on the three-dimensional flow through compressor cascades deals with a row of rotor blades in isolation. Since the distance between the rotor and stator is usually 10 to 20 percent of the blade chord, the aerodynamic interference between them has to be considered for a proper evaluation of the aerothermodynamic performance of the stage. A unified approach to the aerodynamics of the incompressible flow through a stage is presented that uses the lifting-surface theory for a compressor cascade of arbitrary camber and thickness distribution. The effects of rotor-stator interference are represented as a linear function of the rotor and stator flows separately. The loading distribution on the rotor and stator blades and the interference factor are determined concurrently through a matrix iteration process.					
17. Key Words (Suggested by Author(s)) Turbomachines Aerodynamics Cascades			18. Distribution Statement Unclassified - unlimited STAR Category 02		
19. Security Classif. (of this report) Unclassified		20. Security Classif. (of this page) Unclassified		21. No. of pages	
				22. Price*	

National Aeronautics and
Space Administration

SPECIAL FOURTH CLASS MAIL
BOOK



Washington, D.C.
20546

Official Business

Penalty for Private Use, \$300

Postage and Fees Paid
National Aeronautics and
Space Administration
NASA-451

NASA

POSTMASTER: If Undeliverable (Section 158
Postal Manual) Do Not Return
